

Preparation, Properties, and Crystal Structure of New Conjugated Oligomers with a Pendant Ferrocenyl and an End-Capped Pyridine

José A. Mata,[†] Santiago Uriel,[†] Rosa Llusar,[‡] and Eduardo Peris^{*,†}

Departamento de Química Inorgánica y Orgánica and Departamento de Ciencias Experimentales, Universitat Jaume I, E-12080 Castellón, Spain

Received March 14, 2000

New ferrocenyl–pyridine conjugated ligands have been obtained by several routes in which we combined Wittig and Horner–Emmons–Wadsworth (HEW) reactions, the latter showing better results both in yield and selectivity for the *E* isomers. Methylation of the ferrocenyl–pyridyl compounds yields cationic ferrocenyl–pyridinium compounds, whose electronic properties have been studied. The crystal structures of several of the described complexes are reported, showing a conjugated pathway of up to 27 Å.

Introduction

Metal-containing long-chain conjugated systems have emerged as an important category of materials. The impetus for developing these materials is based on the premise that conjugated chains containing metals are expected to possess properties significantly different from those of conventional organic conjugated oligomers. Examples of these properties include electrical conductivity, magnetic behavior, thermal stability, nonlinear optical (NLO) effects, and even superconductivity. Because of the special electronic and chemical properties of ferrocene, many efforts have been directed toward the incorporation of a ferrocene moiety into a polymer,¹ in order to investigate novel properties such as those mentioned above. Besides, the preparation of ferrocenyl conjugated systems offers the possibility of electronic communication between terminal subunits, this being of particular interest in terms of modulating the electronic properties of the material.

Although many studies have been reported in which metallocene-based oligomers are obtained,² there is still a lack of systematic descriptions of synthesis leading to useful starting materials. All the reported metal-containing polymers have in common that they are only conducting if charge carriers can be delocalized over both the metal and the organic fragments.

We and others have used ferrocenyl-based conjugated ligands in order to obtain bimetallic and heterometallic push–pull complexes.³ Most of the problems regarding the synthesis of such complexes are the difficulties found

when trying to increase the conjugated chain in a multistep synthetic procedure. Bildstein et al. have published excellent results regarding the synthesis of ferrocenyl “molecular wires”, in which the metal-to-metal distance reaches up to 40 Å.⁴ Since the electronic and optical responses of the materials seem to be highly influenced by the length of the conjugated chain connecting the electron-donating and electron-accepting termini of the molecule, we focused our efforts on obtaining long-chain oligomers with a pendant ferrocene fragment. We have recently reported the preparation and properties of new conjugated ferrocenyl-based ligands with an end-capped nitrile, with an estimated distance between the iron atom and the nitrile group of up to 23 Å.⁵ These complexes showed interesting electronic and spectroscopic properties that made them good candidates for NLO measurements. However, the step-by-step syntheses of these compounds sometimes are tedious and complicated, and the yields are usually poor.

Some conjugated pyridines with end-capping ferrocene have been reported by Lin et al.,^{3b} and their electronic and coordinative properties have been described. We now report, on the basis of our previous findings, several routes to the preparation of ferrocenyl conjugated compounds with an end-capped pyridine ring. These compounds are obtained by combined Wittig and/or Horner–Emmons–Wadsworth (HEW) reactions.

(3) (a) Mata, J.; Uriel, S.; Peris, E.; Llusar, R.; Houbrechts, S.; Persoons, A. *J. Organomet. Chem.* **1998**, *562*, 197. (b) Lin, J. T.; Wu, J. J.; Li, C.-S.; Wen, K.-J.; Lin, Y. S. *Organometallics* **1996**, *15*, 5028. (c) Togni, A.; Rins, G. *Organometallics* **1993**, *12*, 3368. (d) Doineau, G.; Balavoine, G.; Fillebeen-Khan, T.; Clinet, J. C.; Delaire, J.; Ledoux, I.; Loucif, R.; Puccetti, G. *J. Organomet. Chem.* **1991**, *421*, 299. (e) Lee, I. S.; Lee, S. S.; Chung, Y. K.; Kim, D.; Song, N. W. *Inorg. Chim. Acta* **1998**, *279*, 243. (f) Jayaprakash, K. N.; Ray, P. C.; Matsuoka, I.; Bhadrade, M. M.; Puranik, V. G.; Das, P. K.; Nishihara, H.; Sarklar, A. *Organometallics* **1999**, *18*, 3851. (g) Sakanishi, S.; Badrddwell, D. A.; Couchman, S.; Jeffrey, J. C.; McCleverty, J. A.; Ward, M. D. *J. Organomet. Chem.* **1997**, *528*, 35. (h) Hsung, R. P.; Chidsey, C. E. D.; Sita, L. R. *Organometallics* **1995**, *14*, 4808. (i) Thomas, K. R. J.; Lin, J. T.; Lin, K. J. *Organometallics* **1999**, *18*, 5285.

(4) Hradsky, A.; Bildstein, B.; Schuler, N.; Schottenberger, H.; Jaitner, P.; Ongania, K.-H.; Wurst, K.; Launay, J.-P. *Organometallics* **1997**, *16*, 392.

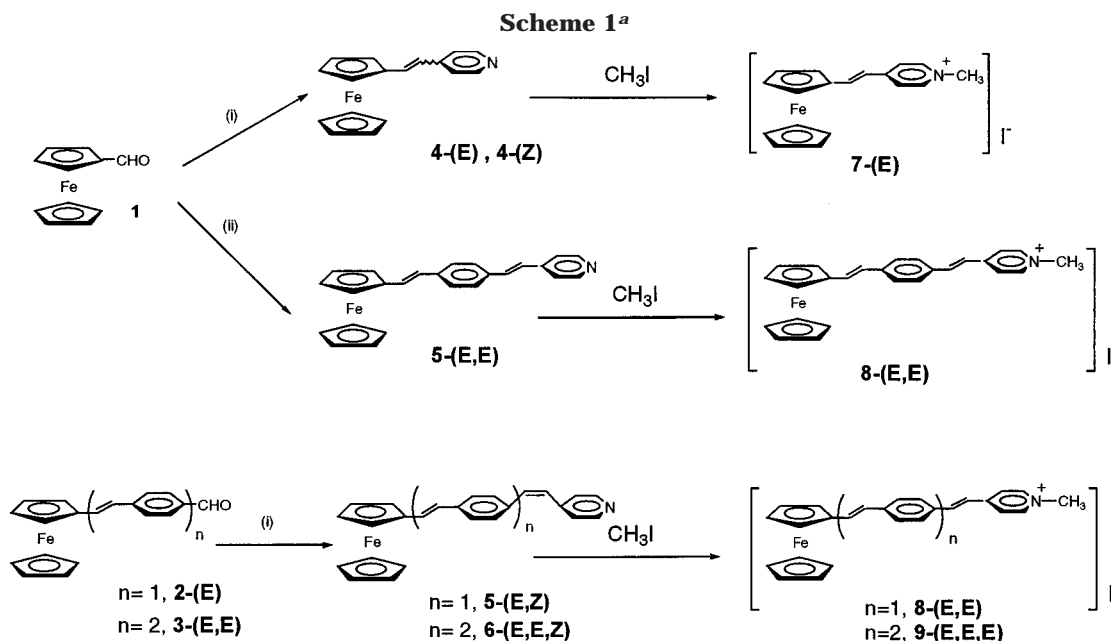
(5) Mata, J. A.; Falomir, E.; Llusar, R.; Peris, E. *J. Organomet. Chem.*, submitted for publication.

[†] Departamento de Química Inorgánica y Orgánica.

[‡] Departamento de Ciencias Experimentales.

(1) (a) Long, N. J. In *Metallocenes: An Introduction to Sandwich Complexes*; Blackwell Science: Oxford, U.K., 1998; Chapter 6. (b) Togni, A.; Hayashi, T. *Ferrocenes*; VCH: New York, 1995; Chapter 10.

(2) (a) Long, N. J.; Martin, A. J.; Vilar, R.; White, A. J. P.; Williams, D. J.; Younus, M. *Organometallics* **1999**, *18*, 4261. (b) Barlow, S.; O'Hare, D. *Chem. Rev.* **1997**, *97*, 637. (c) Zhu, Y.; Clot, O.; Wolf, O.; Yap, G. P. A. *J. Am. Chem. Soc.* **1998**, *120*, 1812. (d) Lavastre, O.; Ollivier, L.; Dixneuf, P. H.; Sibandhit, S. *Tetrahedron* **1996**, *51*, 1683. (e) Colbert, M. C. B.; Lewis, J.; Long, N. J.; Raithby, P. R.; White, A. J. P.; Williams, D. J. *J. Chem. Soc., Dalton Trans.* **1997**, 99. (f) Lavastre, O.; Even, M.; Dixneuf, P. H.; Pacreau, A.; Vairon, J.-P. *Organometallics* **1996**, *15*, 1530.



^a Legend: (i) $[\text{Ph}_3\text{P}^+\text{CH}_2\text{py}]\text{Cl}^-/\text{BuOK}$; (ii) (1) $p\text{-(EtO)}_2\text{P(O)CH}_2\text{C}_6\text{H}_4\text{CH}_2\text{P(O)(OEt)}_2/\text{NaH}$, (2) NaH (3) $p\text{-OHCC}_6\text{H}_4\text{CHO}$.

Methylation of the pyridyl compounds with CH_3I leads to the corresponding *N*-methylpyridinium derivatives. These compounds are very interesting, since the related compound $(E)\text{-}[\text{CpFe}(\eta^5\text{-C}_5\text{H}_4)\text{CH}=\text{CHC}_5\text{H}_4\text{N}^+\text{CH}_3]\text{I}^-$ has proved to be one of the most effective NLO chromophores reported to date.⁶ The electrochemistry of the compounds and the electronic spectra are also investigated.

Results and Discussion

Most of the ferrocenyl-based oligomers reported to date have been obtained by conventional Wittig reactions, but these reactions usually lead to the formation of *E* and *Z* isomer mixtures.^{4,7} Several authors have reported the advantages of the *E* type isomers over the *Z* type for effective electronic coupling.^{7c,8} The lack of coplanarity between donor and acceptor groups in the *Z* isomers leads to a decrease in their electronic communication. In addition, the reduction of the through-space distance (in the *Z*-type) between donor and acceptor results in a lower change in dipole per unit charge separation. Since most of the time the aim of the synthetic procedures is to obtain linear oligomers with effective electronic coupling, the *E* isomers are the ones that are mainly pursued, but the separation of the mixtures of the *E* and *Z* isomers is not always easy. We recently reported the preparation and characterization of new ferrocenyl-based ligands with an end-capping nitrile. The syntheses of these complexes showed an

increasing difficulty upon lengthening the connection between the ferrocenyl and nitrile units and, in the case of the longest ligand, this being $(E,E,E)\text{-}(\eta^5\text{-C}_5\text{H}_5)\text{Fe}(\eta^5\text{-C}_5\text{H}_4)\text{CH}=\text{CH}(\text{C}_6\text{H}_4)\text{CH}=\text{CH}(\text{C}_6\text{H}_4)\text{CH}=\text{CH}(\text{C}_6\text{H}_4)\text{CN}$, the synthetic procedure led to such a low yield that only spectroscopic characterization of the compound could be achieved.

In the synthesis of the new ferrocenyl compounds connected to a pyridyl unit by a conjugated chain, we used conventional Wittig and HEW reactions, as shown in Scheme 1. The ferrocenyl aldehydes **2-(E)** and **3-(E,E)** were obtained according to the methods reported in the literature.^{3a,5} Compounds **4-(E)** and **4-(Z)** have already been reported, and their coordination capabilities and electronic properties have been extensively described.^{3a,e} The olefination of the aldehyde **2-(E)** by conventional Wittig reaction leads to a mixture of *Z* and *E* isomers, the *E* isomer being the major one. However, the olefination of the aldehyde **3-(E,E)** leads selectively to the formation of the *Z* isomer **6-(E,E,Z)**.

The use of *p*-xylenebis(diethylphosphonate) in the HEW reactions leads unambiguously to the formation of the *E* isomer **5-(E,E)**. However, the same reaction did not lead to favorable results in the case of the olefination of the aldehyde **3-(E,E)** for reasons that we still do not know. In fact, we believe that this unfavorable result may be due to the low solubility of compound **6-(E,E,E)**, which would be formed by this procedure. This low solubility, probably due to the rigid-row geometry derived from the all-*E* configuration, complicates the characterization of the compound (**6-(E,E,E)**, if formed) by conventional methods and, furthermore, would explain the loss of the aforementioned compound during the extraction of compounds made in the last step of the olefination reaction. A similar effect was reported by Bildstein et al.⁴ when elongating the conjugated chains of some permethylated ferrocenyl complexes. Conventional methods for the isomerization of the *Z* to *E* double bonds (such as using *N*-bromosuccinimide and

(6) Marder, S. R.; Perry, J. W.; Tiemann, B. G.; Schaefer, W. P. *Organometallics* **1991**, *10*, 1896.

(7) (a) Balavoine, G. G. A.; Daran, J.-C.; Iftime, G.; Lacroix, P. G.; Manoury, E.; Delaire, A.; Maltey-Fanbton, I. J.; Nakatani, K. *Organometallics* **1999**, *18*, 21. (b) Bhadbhade, M. M.; Das, A.; Jeffrey, J. C.; McCleverty, J. A.; Navas-Badiola, J. A.; Ward, M. D. *J. Chem. Soc., Dalton Trans.* **1995**, 2769. (c) Thomas, K. R. J.; Lin, J. T.; Wen, Y. S. *J. Organomet. Chem.* **1999**, *575*, 301. (d) Bunting, H. E.; Green, M. L. H.; Marder, S. R.; Thompson, M. E.; Bloor, D.; Kolinsky, P. V.; Jones, R. J. *Polyhedron* **1992**, *11*, 1489.

(8) (a) Houlton, A.; Miller, J. R.; Silver, J.; Jassim, N.; Axon, T. L.; Bloor, D.; Cross, G. H. *Inorg. Chim. Acta* **1993**, *205*, 67. (b) Calabrese, J. C.; Cheng, L.; Green, J. C.; Marder, S. R.; Tam, W. *J. Am. Chem. Soc.* **1991**, *113*, 7227.

I₂ or with basic alumina) were tried, but no conversion was observed.

Methylation of the pyridine complexes led to the corresponding cationic ferrocenyl–methyl–pyridinium salts. The corresponding methylated salts showed an *E* conformation even when the starting pyridyl complex corresponded to the *Z* conformation, this indicating that an isomerization process had occurred during the methylation. This effect was especially observed for the reactions of **5**-(*E,Z*) to **8**-(*E,E*) and **6**-(*E,E,Z*) to **9**-(*E,E,E*).

The electronic absorption spectra of the ferrocenylpyridyl compounds **4**–**6** and the ferrocenyl–methyl–pyridinium salts **7**–**9** were taken in different solvents. In general, the electronic absorption spectra of the neutral compounds show two prominent bands at 300 and 370 nm assigned to the π – π^* transitions, according to the reported data in the literature for substituted ferrocenyl compounds.^{3e,9} The weaker band at about 450 nm is assigned to a ferrocenyl-based MLCT band. Another weak band at higher wavelengths (about 500 nm), assigned to a d–d transition, is only discernible in some cases as a shoulder of the other MLCT band. The MLCT band is strongly influenced by the nature of the ancillary ligand, showing a hypsochromic shift upon lengthening the conjugated chain. This result is not surprising, since the more intense π – π^* band also shows a clear dependence on the nature of the ligand, probably because elongating the conjugation length lowers the energy of the π^* orbital. However, a nonlinear increase in λ_{max} is observed when going from **7**-(*E*) to **8**-(*E,E*) and **9**-(*E,E,E*), suggesting different net contributions for each additional phenylene–vinylene subunit. These data (although limited to only three points) suggest that an effective limit for conjugation may be envisaged, this being supported by the results reported by Hsung et al.,^{3h} where again, a nonlinear shift of λ_{max} is observed upon elongating the chain of a series of ferrocenyl-based phenylethynyl oligomers. The methylation of the complexes to the cationic methylpyridinium compounds increases the λ_{max} values by 40 nm (π – π^*) and 60 nm (MLCT), confirming that the generation of the cationic site located on the nitrogen atom of the pyridine results in an inductive electron-accepting character.

Ferrocenyl–pyridine compounds show moderate solvatochromic behavior. This result gives us an idea of the dipole moments in the ground and in the excited states, which have a direct relation to hyperpolarizability. The π – π^* charge-transfer band shifts upon changing the solvent from CHCl₃ to MeOH. These hypsochromic shifts mean that the dipole moment in the excited state is lower than in the ground state. In addition, this effect is greater in the cases where all the double bonds are *E*.

The electrochemical data for these compounds were measured using the same setup, except the ferrocenyl–methyl–pyridinium salts that were measured in acetone instead of CH₂Cl₂ because of the low solubility of these salts in the latter solvent. In all cases we observed the chemically reversible ferrocene/ferrocenium couple with $i_{\text{p,a}}/i_{\text{p,c}} \approx 1$. As previously reported, the half-wave

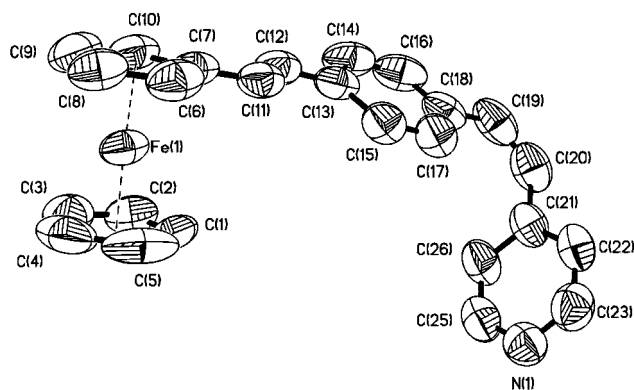


Figure 1. Molecular structure of **5**-(*E,Z*) showing the atom-numbering scheme. Hydrogen atoms are omitted for clarity. Distances: Fe–N(through space) = 9.74 Å and Fe–N(through bonds) = 18.74 Å. Torsion angle: Cp–Cp-(substituted) = 2.39(0.35)°. Thermal ellipsoids are drawn at 50% probability.

potential of the ferrocenyl moieties for the aldehyde derivatives **1**, **2**-(*E*), and **3**-(*E,E*) and for pyridyl derivatives **4**-(*E*) and **7**-(*E*) are more anodic than that measured for ferrocene, indicating some degree of electron transfer between the iron center and the electron-accepting fragment.⁵ Elongation of the chain promotes a decrease in the redox potential, probably due to the stabilization of the positive charge of the oxidized species along the conjugated chain. This cathodic shift is particularly significant (ca. 200 mV) when going from compound **7**-(*E*) to **8**-(*E,E*) but is much less important when adding a new vinyl–phenylene subunit to obtain **9**-(*E,E,E*).

Humphrey has reported that stepwise elongation of the conjugated chain in ruthenium acetylides leads to an increase in the NLO responses of the material, but this increase is gradually reduced until an asymptotic or limit situation is achieved, in which elongation of the chain does not lead to any further increase in the NLO responses.¹² This observation, together with our results, suggests that conjugation may actually reach a limiting effective length.

The ORTEP drawings and selected bond distances and angles of the ferrocenyl–vinylene–phenylene–pyridyl and methylpyridinium (as PF₆ salts) complexes **5**-(*E,Z*), **8**-(*E,E*), and **9**-(*E,E,E*) are displayed in Figures 1–3, respectively. The molecular structure of compound **5**-(*E,E*) was also resolved, being very similar to that of **8**-(*E,E*) (all data are included in the Supporting Information). In all cases the two cyclopentadienyl rings are slightly tilted (2.4–6.5°) with respect to each other. The iron distances to the substituted and unsubstituted rings and the C–C distances within these rings lie in the expected ranges. **5**-(*E,E*) presents a disorder in a 1:1 ratio with regard to the orientation of the trans olefinic moieties. This kind of disorder has been observed in similar molecules.^{3g,4} Except for compound **5**-(*E,Z*), with a *Z* olefinic geometry, the phenylene and pyridyl rings are roughly coplanar with the substituted

(10) Blanchard-Desce, M.; Runser, C.; Fort, A.; Barzoukas, M.; Lehn, J. M.; Bloy, V.; Alain, V. *Chem. Phys.* **1995**, *199*, 253.

(11) (a) SAINT, version 5.0; Bruker Analytical X-ray Systems, Madison, WI. (b) Sheldrick, G. M. SADABS Empirical Absorption Program; University of Göttingen, Göttingen, Germany, 1996.

(12) Whittall, I. R.; McDonagh, A. M.; Humphrey, M. G.; Samoc, M. *Adv. Organomet. Chem.* **1999**, *43*, 349.

(9) (a) Schumm, J. S.; Pearson, D. L.; Tom, J. M. *Angew. Chem., Int. Ed. Engl.* **1994**, *33*, 1360. (b) Hsung, R. P.; Chidsey, C. E. D.; Sita, L. R. *Organometallics* **1995**, *14*, 4808.

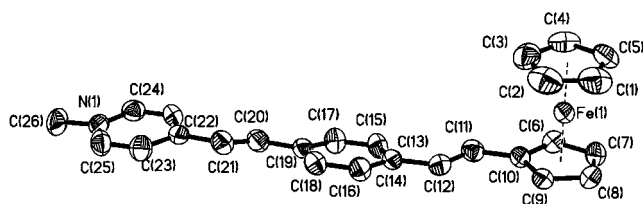


Figure 2. Molecular structure of **8-(E,E)** showing the atom-numbering scheme. Hydrogen atoms are omitted for clarity. The counteranion PF_6 has also been omitted for clarity. Distances: Fe–N(through space) = 14.41 Å and Fe–N(through bonds) = 18.77 Å. Torsion angles: Cp–Cp(substituted) = 5.36(0.41)°; Ph–Cp(substituted) = 11.96(0.43)°; Py–Cp(substituted) = 1.91(0.36)°. Thermal ellipsoids are drawn at 50% probability.

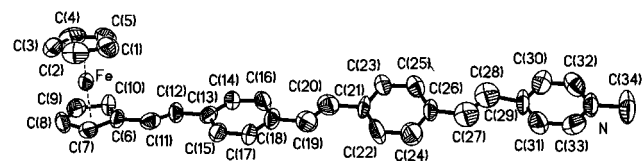


Figure 3. Molecular structure of **9-(E,E,E)** showing the atom-numbering scheme. Hydrogen atoms are omitted for clarity. The counteranion PF_6 has also been omitted for clarity. Distances: Fe–N(through space) = 21.03 Å and Fe–N(through bonds) = 27.13 Å. Torsion angles: Cp–Cp(substituted) = 6.49(1.08)°; Ph1–Cp(substituted) = 8.73(0.94)°; Ph2–Cp(substituted) = 29.66(0.74)°; Py–Cp(substituted) = 18.77(0.88)°. Thermal ellipsoids are drawn at 50% probability.

Cp ring. In **5-(E,E)** the through-space Fe–N distance equals 14.8 Å and the sum of the bond lengths corresponding to the conjugation pathway from Fe to N is 18.88 Å. Almost the same through-space distance between the Fe and N atoms is observed for the methylated compound **8-(E,E)** (14.4 Å), indicating that no significant modification of the conjugated backbone has occurred upon methylation.

The pyridinium compound **9-(E,E,E)** shows Fe–N distances of 21.03 Å (through space) and 27.13 Å (through conjugated bonds). A clear loss of coplanarity with respect to the substituted Cp ring is observed, which may be due to solid-state effects, although a loss of coplanarity cannot be discarded in solution, regarding the electronic spectra and electrochemical behavior of the compound.

It is important to point out that both ferrocenyl–pyridinium complexes **8-(E,E)** and **9-(E,E,E)** show an eclipsed disposition of the Cp rings of the ferrocenyl fragment, in contrast to the staggered disposition in the pyridyl complexes **5-(E,E)** and **5-(E,Z)**. This effect has already been described for other systems, and it has been pointed out that the electronic perturbation induced by oxidation of the iron atom or, in our case, the effective electronic communication from the positively charged pyridinium moiety and the ferrocenyl fragment may promote this change in the relative conformation of the two Cp rings in order to relieve steric strain induced by electronic perturbation.^{1b}

Experimental Section

NMR spectra were recorded on Varian Innova 300 and 500 MHz instruments, using CDCl_3 as solvent unless otherwise

stated. IR spectra were recorded on a Perkin-Elmer System 2000 FT-IR using NaCl pellets. Electronic absorption spectra were obtained on a Shimadzu UV-1603 spectrophotometer. Cyclic voltammetry experiments were performed with a Echochemie PGSTAT 20 electrochemical analyzer. All measurements were carried out at room temperature with a conventional three-electrode configuration consisting of platinum working and auxiliary electrodes and a Ag/AgCl reference electrode containing aqueous 3 M KCl. The supporting electrolyte was 0.1 M tetrabutylammonium hexafluorophosphate. All potential data reported are not corrected for the junction potential. Electrospray mass spectra were recorded using a Micromass Quattro LC instrument, using CH_3CN and/or CH_3OH as the mobile-phase solvent. The samples were added to give a mobile phase of approximate concentration 0.1 mM. Ferrocenealdehyde (**1**) was used as purchased (Aldrich); (*E*)-(ferrocenylethenyl)benzaldehyde (**2-(E)**) and (*E,E*)-(ferrocenylethenyl)-4-formylstilbene (**3-(E,E)**) were obtained according to literature methods^{3a,5} or by the method reported by Bildstein et al. for the permethylated ferrocenyl derivatives.⁴ **7-(E)** was also obtained by the method described in the literature.⁶

Synthesis of {(*E,Z*)-(η⁵-C₅H₅)Fe(η⁵-C₅H₄)(CH=CH)(C₆H₄)-(CH=CH)(C₅H₄N)} (5-(E,Z)**).** To an ice-cold solution of *p*-(triphenylphosphino)methylpyridinium iodide (1 g, 2.6 mmol) in THF (75 mL) was added potassium *tert*-butoxide (393 mg, 3.5 mmol), and the resulting solution was stirred for 30 min at 0 °C and for 45 min at room temperature. The aldehyde **2-(E)** (758 mg, 2.4 mmol) was added at 0 °C, and the resulting solution was stirred overnight at room temperature. After the solvent was removed under reduced pressure, the product was extracted with $\text{CH}_2\text{Cl}_2/\text{H}_2\text{O}/\text{NaHCO}_3$ and dried over MgSO_4 . The title compound was purified by column chromatography on silica gel, washing with hexane/ CH_2Cl_2 (1:1) first and using CH_2Cl_2 as eluent. Recrystallization from CH_2Cl_2 /hexane mixtures afforded pure **5-(E,Z)**. Yield: 15%. ¹H NMR (500 MHz, CDCl_3): δ 8.51 (d, 2H, ³*J*_{H–H} = 4.5 Hz, C₅H₄N); 7.19 (m, 4H, C₅H₄N, C₆H₄); 7.32 (d, 2H, ³*J*_{H–H} = 8.5 Hz, C₆H₄); 6.89 (d, 1H, ³*J*_{H–H} = 16.0 Hz, CH=CH); 6.67 (d, 1H, ³*J*_{H–H} = 16.0 Hz, CH=CH); 6.75 (d, 1H, ³*J*_{H–H} = 12.0 Hz, CH=CH); 6.49 (d, 1H, ³*J*_{H–H} = 12.0 Hz, CH=CH); 4.47 (t, 2H, ³*J*_{H–H} = 1.8 Hz, C₅H₄); 4.30 (t, 2H, ³*J*_{H–H} = 1.8 Hz, C₅H₄); 4.15 (s, 5H, C₅H₅). ¹³C NMR (300 MHz, CDCl_3): δ 67.6, 69.8 (4C, C₅H₄); 69.9 (5C, C₅H₅); 83.7 (1C_q, C₅H₄); 124.1, 125.9, 126.3, 127.6, 128.3, 129.8, 134.3, 150.4 (12C, CH=CH and C₆H₄); 134.9, 138.1, 145.8 (3C_q, C₆H₄). IR (cm^{−1}): 1592 (w), 1411 (w), 815 (w). Anal. Calcd for **5-(E,Z)**, C₂₅H₂₁FeN, *M*_w = 391.30: C, 76.7; H, 5.41; N, 3.58. Found: C, 75.9; H, 5.49; N, 3.48. Electrospray MS (*m/z* (fragment)): cone 70 V, 392 (*M*⁺); cone 110 V, 392 (*M*⁺), 326 (*M*⁺ – Cp).

Synthesis of {(*E,E*)-(η⁵-C₅H₅)Fe(η⁵-C₅H₄)(CH=CH)(C₆H₄)-(CH=CH)(C₅H₄N)} (5-(E,E)**).** To an ice-cold solution of *p*-xylenebis(diethylphosphonate) (2.0 g, 5.3 mmol) in THF (75 mL) was added sodium hydride (212 mg, 5.3 mmol), and the resulting solution was stirred for 45 min at 0 °C and 60 min at room temperature. The aldehyde **1** (1.1 g, 5.0 mmol) was added at 0 °C and the resulting solution was stirred for 5 h at room temperature. Then, sodium hydride (212 mg, 5.3 mmol) was added at 0 °C and the mixture stirred for 45 min at room temperature. Finally, 4-pyridinecarboxaldehyde (643 mg, 6.0 mmol) was added, and the reaction mixture was stirred overnight at room temperature. After the solvent was removed under reduced pressure, the product was extracted with $\text{CH}_2\text{Cl}_2/\text{H}_2\text{O}/\text{NaHCO}_3$ and dried over MgSO_4 . The title compound was purified by column chromatography on silica gel, washing with hexane/ CH_2Cl_2 (1:4) first and using CH_2Cl_2 /acetone (1:1) as eluent. Recrystallization from CH_2Cl_2 /hexane mixtures afforded pure compound **5-(E,E)**. Yield: 35%. ¹H NMR (500 MHz, CDCl_3): δ 8.60 (s, 2H, C₅H₄N); 7.38 (d, 2H, ³*J*_{H–H} = 4.0 Hz, C₅H₄N); 7.51 (d, 2H, ³*J*_{H–H} = 8.0 Hz, C₆H₄); 7.45 (d, 2H, ³*J*_{H–H} = 7.5 Hz, C₆H₄); 7.29 (d, 1H, ³*J*_{H–H} = 16.0 Hz, CH=CH); 7.02 (d, 1H, ³*J*_{H–H} = 16.0 Hz, CH=CH); 6.94 (d, 1H, ³*J*_{H–H}

Table 1. Crystallographic Data

	5-(<i>E,Z</i>)	5-(<i>E,E</i>)	8-(<i>E,E</i>)PF ₆	9-(<i>E,E,E</i>)PF ₆
empirical formula	C ₂₅ H ₂₁ FeN	C ₂₅ H ₂₁ FeN	C ₂₆ H ₂₄ F ₆ FeNP	C ₃₄ H ₃₀ FeNPF ₆
fw	391.28	391.28	551.28	653.41
temp (K)	293(2)	293(2)	293(2)	293(2)
wavelength (Å)	0.710 73	0.710 73	0.710 73	0.710 73
cryst syst	monoclinic	monoclinic	monoclinic	monoclinic
space group	<i>P</i> 2 ₁ / <i>c</i>	<i>P</i> 2 ₁	<i>P</i> 2 ₁ / <i>c</i>	<i>P</i> 2 ₁ / <i>c</i>
<i>a</i> (Å)	17.7672(18)	6.2814(4)	12.0649(9)	14.1378(9)
<i>b</i> (Å)	10.0114(9)	7.7253(6)	15.7470(12)	17.6844(11)
<i>c</i> (Å)	11.3680(11)	19.3917(14)	12.5267(9)	12.6401(8)
α (deg)	90	90	90	90
β (deg)	106.027(2)	95.394(2)	95.150(2)	110.748(2)
γ (deg)	90	90	90	90
<i>V</i> (Å ³)	1943.5(3)	936.83(12)	2370.3(3)	2955.3(3)
<i>Z</i>	4	4	4	4
calcd density (Mg m ⁻³)	1.337	1.387	1.545	1.469
abs coeff (mm ⁻¹)	0.784	0.813	0.767	0.628
no. of rflns collected	7085	4833	11387	11043
final <i>R</i> indices (<i>I</i> > 2σ(<i>I</i>))	<i>R</i> 1 = 0.0318, w <i>R</i> 2 = 0.0835	<i>R</i> 1 = 0.0411, w <i>R</i> 2 = 0.0896	<i>R</i> 1 = 0.0548, w <i>R</i> 2 = 0.1356	<i>R</i> 1 = 0.1035, w <i>R</i> 2 = 0.3046
goodness of fit on <i>F</i> ²	1.023	0.974	1.060	1.232

= 16.0, CH=CH); 6.71 (d, 1H, ³*J*_{H-H} = 16.0 Hz, CH=CH); 4.49 (s, 2H, C₅H₄); 4.32 (s, 2H, C₅H₄); 4.16 (s, 5H, C₅H₅). ¹³C NMR (300 MHz, CDCl₃): δ 67.7, 69.7 (4C, C₅H₄); 69.7 (5C, C₅H₅); 83.7 (1C_q, C₅H₄); 121.4, 125.8, 125.9, 126.7, 128.0, 128.6, 133.5, 150.7 (12C, CH=CH and C₆H₄); 135.1, 139.1, 145.3 (3C_q, C₆H₄). IR (cm⁻¹): 1588 (w), 1409 (w), 821 (w). Anal. Calcd for 5-(*E,E*), C₂₅H₂₁FeN, *M*_w = 391.30: C, 76.7; H, 5.41; N, 3.58. Found: C, 76.5; H, 5.43; N, 3.56. Electrospray MS (*m/z* (fragment)): cone 70 V, 392.1 (M⁺); cone 110 V, 392.1 (M⁺), 326.1 (M⁺ - Cp).

Synthesis of {(E,E,Z)-(η⁵-C₅H₅)Fe(η⁵-C₅H₄)(CH=CH)-(C₆H₄)(CH=CH)(C₆H₄)(CH=CH)(C₅H₄N)} (6-(E,E,Z)). This compound was obtained by following the general procedure described for 5-(*E,Z*) and using the aldehyde 3-(*E,E*) (1 g, 2.4 mmol) instead of 2-(*E*). The purification was carried out by column chromatography on silica gel using hexane/CH₂Cl₂ (1:1) as eluent. Yield: 25%. ¹H NMR (300 MHz, CDCl₃): δ 8.50 (s, 2H, C₅H₄N); 7.54–7.40 (m, 6H, C₆H₄); 7.25–7.16 (m, 4H, C₆H₄, C₅H₄N); 7.10 (d, 1H, ³*J*_{H-H} = 16.5 Hz, CH=CH); 7.09 (d, 1H, ³*J*_{H-H} = 16.5 Hz, CH=CH); 6.91 (d, 1H, ³*J*_{H-H} = 16.2 Hz, CH=CH); 6.71 (d, 1H, ³*J*_{H-H} = 15.9 Hz, CH=CH); 6.78 (d, 1H, ³*J*_{H-H} = 12.3 Hz, CH=CH); 6.51 (d, 1H, ³*J*_{H-H} = 12.3 Hz, CH=CH); 4.49 (s, 2H, C₅H₄); 4.31 (s, 2H, C₅H₄); 4.16 (s, 5H, C₅H₅). ¹³C NMR (300 MHz, CDCl₃): δ 67.6, 69.8 (4C, C₅H₄); 69.9 (5C, C₅H₅); 83.9 (1C_q, C₅H₄); 126.2, 126.7, 127.0, 127.2, 127.5, 127.8, 127.9, 128.0, 129.5, 129.8, 134.2, 150.4 (18C, CH=CH and C₆H₄); 135.8, 136.2, 137.7, 138.1, 145.7 (5C_q, C₆H₄). Anal. Calcd for 6-(*E,E,Z*), C₃₃H₂₇FeN, *M*_w = 493.43: C, 80.3; H, 5.52; N, 2.84. Found: C, 80.7; H, 5.61; N, 2.88. Electrospray MS (*m/z* (fragment)): cone 70 V, 494 (M⁺), cone 110 V, 494 (M⁺), 428 (M⁺ - Cp).

Synthesis of {(E,E)-(η⁵-C₅H₅)Fe(η⁵-C₅H₄)(CH=CH)(C₆H₄)-(CH=CH)(C₅H₄N)CH₃}PF₆ (8-(E,E)). To a solution of 5-(*E,Z*) or 5-(*E,E*) (100 mg, 0.26 mmol) in toluene (45 mL) was added iodomethane (63.9 mg, 0.45 mmol), and the reaction mixture was warmed to 100 °C for 3 days. After the solution was cooled to room temperature, a wine red solid was obtained. This compound was purified by column chromatography on silica gel, washing with CH₂Cl₂ and eluting with acetone or a solution of KPF₆ in acetone. Recrystallization from acetone/hexane mixtures afforded the pure compound 8-(*E,E*)PF₆. Yield: 85%. ¹H NMR for 8-(*E,E*)PF₆ (300 MHz, d₆-acetone): δ 8.81 (d, 2H, ³*J*_{H-H} = 6.5 Hz, C₅H₄N); 8.37 (d, 2H, ³*J*_{H-H} = 6.5 Hz, C₅H₄N); 7.90 (d, 2H, ³*J*_{H-H} = 8.5 Hz, C₆H₄); 7.74 (d, 2H, ³*J*_{H-H} = 8.0 Hz, C₆H₄); 8.14 (d, 1H, ³*J*_{H-H} = 16.0 Hz, CH=CH); 7.66 (d, 1H, ³*J*_{H-H} = 16.5 Hz, CH=CH); 7.32 (d, 1H, ³*J*_{H-H} = 16.0 Hz, CH=CH); 6.99 (d, 1H, ³*J*_{H-H} = 16.0 Hz, CH=CH); 4.73 (t, 2H, ³*J*_{H-H} = 1.5 Hz, C₅H₄); 4.48 (t, 2H, ³*J*_{H-H} = 1.5 Hz, C₅H₄); 4.29 (s, 5H, C₅H₅); 4.57 (s, 3H, CH₃). ¹H NMR for 8-(*E,E*)I (300 MHz, d₆-acetone): δ 8.49 (d, 2H, ³*J*_{H-H} = 6.3 Hz,

C₅H₄N); 8.05 (d, 2H, ³*J*_{H-H} = 6.9 Hz, C₅H₄N); 7.75 (d, 2H, ³*J*_{H-H} = 8.4 Hz, C₆H₄); 7.63 (d, 2H, ³*J*_{H-H} = 9.3 Hz, C₆H₄); 7.86 (d, 1H, ³*J*_{H-H} = 16.2 Hz, CH=CH); 7.40 (d, 1H, ³*J*_{H-H} = 16.2 Hz, CH=CH); 7.18 (d, 1H, ³*J*_{H-H} = 16.2 Hz, CH=CH); 6.88 (d, 1H, ³*J*_{H-H} = 16.2 Hz, CH=CH); 4.62 (s, 2H, C₅H₄); 4.42 (s, 2H, C₅H₄); 4.22 (s, 5H, C₅H₅); 4.24 (s, 3H, CH₃). Anal. Calcd for 8-(*E,E*), C₂₆H₂₄FeNPF₆, *M*_w = 551.29: C, 56.6; H, 4.39; N, 2.54. Found: C, 57.1; H, 4.54; N, 2.48. Electrospray MS (*m/z* (fragment)): cone 70 V, 406 (M⁺), cone 130 V, 406 (M⁺), 391 (M⁺ - CH₃).

Synthesis of {(E,E,E)-(η⁵-C₅H₅)Fe(η⁵-C₅H₄)(CH=CH)-(C₆H₄)(CH=CH)(C₆H₄)(CH=CH)(C₅H₄N)CH₃}PF₆ (9-(E,E,E)). This compound was obtained by following the general procedure described for 8-(*E,E*) and using 6-(*E,E,Z*) (100 mg, 0.20 mmol) instead of 5-(*E,Z*) or 5-(*E,E*). Yield: 80%. ¹H NMR (300 MHz, d₆-acetone): δ 8.83 (d, 2H, ³*J*_{H-H} = 6.3 Hz, C₅H₄N); 8.26 (d, 2H, ³*J*_{H-H} = 6.3 Hz, C₅H₄N); 8.03 (d, 1H, ³*J*_{H-H} = 16.2 Hz, CH=CH); 7.80 (d, 2H, ³*J*_{H-H} = 8.1 Hz, C₆H₄); 7.73 (d, 2H, ³*J*_{H-H} = 7.8 Hz, C₆H₄); 7.61 (d, 2H, ³*J*_{H-H} = 8.4 Hz, C₆H₄); 7.52 (m, 3H, C₆H₄, CH=CH); 7.37 (d, 1H, ³*J*_{H-H} = 16.5 Hz, CH=CH); 7.31 (d, 1H, ³*J*_{H-H} = 16.5 Hz, CH=CH); 7.06 (d, 1H, ³*J*_{H-H} = 16.2 Hz, CH=CH); 6.81 (d, 1H, ³*J*_{H-H} = 16.2 Hz, CH=CH); 4.56 (s, 2H, C₅H₄); 4.31 (s, 2H, C₅H₄); 4.14 (s, 5H, C₅H₅); 4.46 (s, 3H, CH₃). Anal. Calcd for 9-(*E,E,E*), C₃₄H₃₀FeNPF₆, *M*_w = 653.43: C, 62.5; H, 4.63; N, 2.14. Found: C, 62.9; H, 4.57; N, 2.19. Electrospray MS (*m/z* (fragment)): cone 70 V, 508 (M⁺); cone 160 V, 508 (M⁺), 493 (M⁺ - CH₃), 428 (M⁺ - Cp - CH₃).

X-ray Diffraction Studies. Single crystals were grown by slow diffusion of hexane into concentrated CH₂Cl₂ solutions and mounted on a glass fiber in a random orientation. Data collection was performed at room temperature on a Siemens Smart CCD diffractometer using graphite-monochromated Mo Kα radiation (λ = 0.710 73 Å) with a nominal crystal to detector distance of 4.0 cm. A hemisphere of data was collected on the basis of three ω-scan runs (starting ω = -28°) at values φ = 0, 90, and 180° with the detector at 2θ = 28°. At each of these runs, frames (606, 435, and 230, respectively) were collected at 0.3° intervals and 40 s per frame for 5-(*E,Z*) and 5-(*E,E*) and 60 s per frame for 8-(*E,E*) and 9-(*E,E,E*). Space group assignments are based on systematic absences, *E* statistics, and successful refinement of the structures. Structures were solved by direct methods with the aid of successive difference Fourier maps and were refined using the SHELXTL 5.1 software package. All non-hydrogen atoms were refined anisotropically. Hydrogen atoms were assigned to ideal positions and refined using a riding model. Details of the data collection and cell dimensions are given in Table 1.

The diffraction frames were integrated using the SAINT package and corrected for absorption with SADABS.¹²

Acknowledgment. We thank the CICYT (PB98-1044) and BANCAIXA (P1B98-07) for financial support. We also thank the Generalitat Valenciana for a fellowship (J.A.M.).

Supporting Information Available: Tables of crystallographic data and structure refinement details, atomic coor-

dinates with equivalent isotropic displacement parameters, anisotropic displacement parameters, bond lengths and angles, anisotropic displacement parameters, and hydrogen coordinates with isotropic displacement parameters. This material is available free of charge via the Internet at <http://pubs.acs.org>.

OM000228V